A Concerted Structural Transition in the Plasminogen Activator Inhibitor-1 Mechanism of Inhibition†

Grant E. Blouse,‡,§ Michel J. Perron,‡ Jannah H. Thompson,‡ Duane E. Day,‡ Chad A. Link,‡ and Joseph D. Shore*,‡,§

Henry Ford Health Sciences Center, Division of Biochemical Research, One Ford Place 5-D, Detroit, Michigan 48202, and Wayne State University School of Medicine, Department of Pharmacology, 540 E. Canfield, Detroit, Michigan 48201

Received April 15, 2002; Revised Manuscript Received August 14, 2002

ABSTRACT: The inhibition mechanism of serpins requires a change in structure to entrap the target proteinase as a stable acyl−enzyme complex. Although it has generally been assumed that reactive center loop insertion and associated conformational change proceeds in a concerted manner, this has not been demonstrated directly. Through the substitution of tryptophan with 7-azatryptophan and an analysis of transient reaction kinetics, we have described the formation of an inhibited serpin−proteinase complex as a single concerted transition of the serpin structure. Replacement of the four tryptophans of plasminogen activator inhibitor type-1 (PAI-1) with the spectrally unique analogue 7-azatryptophan permitted observations of conformational changes in the serpin but not those of the proteinase. Formation of covalent acyl−enzyme complexes, but not noncovalent Michaelis complexes, with tissue-type plasminogen activator (t-PA) or urokinase (u-PA) resulted in rapid decreases of fluorescence coinciding with insertion of the reactive center loop and expansion of β-sheet A. Insertion of an octapeptide consisting of the P14−P7 residues of the reactive center loop into β-sheet A produced the same conformational change in serpin structure measured by 7-azatryptophan fluorescence, suggesting that introduction of the proximal loop residues induces the structural rearrangement of the serpin molecule. The atom specific modification of the tryptophan indole rings through analogue substitution produced a proteinase specific effect on function. The reduced inhibitory activity of PAI-1 against t-PA but not u-PA suggested that the mechanism of loop insertion is sensitive to the intramolecular interactions of one or more tryptophan residues.

Serpins are a large superfamily of proteins which includes the circulating serine proteinase inhibitors that play central roles in processes as varied as blood coagulation, fibrinolysis, complement activation, matrix remodeling, inflammation, and also several inhibitors of cysteine proteinases and noninhibitory serpins with diverse functions ranging from chaperones to hormone transport (*1*). All serpins share a highly conserved tertiary structure consisting of three β-sheets (A, B, and C), 7−9 α-helices, and an exposed flexible reactive center loop (RCL) comprising residues P16−P10′. Unlike other proteinase inhibitor families, which function by a "lock-and-key" mechanism in which the RCL is presented to the proteinase in a canonical conformation as a tight binding substrate analogue, serpins employ a highly efficient suicide substrate mechanism by kinetically trapping their target proteinases in stoichiometric covalent acyl−enzyme complexes (*2*).

The serpin inhibitory mechanism is dependent on an extensive conformational change known as the "stressed" to "relaxed" (S → R) transition in which the RCL undergoes rapid insertion into β-sheet A following hydrolysis of the P1−P1′ scissile bond, which traps the proteinase (*3*−*7*). Reversibility of the enzyme inhibition reaction is thus prevented by a large translocation of the covalently bound proteinase, rapidly separating the P1 and P1′ residues by approximately 70 Å (*8*, *9*). The final serpin−proteinase complex is stabilized by complete insertion of the RCL, which results in a distortion of the catalytic triad and a large portion of the proteinase structure (*5*−*10*). A report using [^{1}H-^{15}N] HSQ NMR corroborates this notion and suggests that steric compression and the distortion of the proteinase structure is the basis for the kinetic trapping of the acyl−enzyme intermediate (*11*). Recently solved structures of the initial Michaelis complex (*12*) and the final, inhibited serpin−proteinase complex (*9*) have been used to propose mechanistic postulates for serpin action and the conformational changes during loop insertion. However, direct biochemical evidence supporting the proposed sequence of conformational transitions that define the serpin mechanism and the serpin−proteinase interaction is limited. Various approaches using crystallography (*3*, *9*, *12*), site-specific mutagenesis (*13*−*15*), steady-state fluorescence resonance energy transfer (*16*), and fluorescent labeling of specific RCL residues (*4*) (*17*−*19*) have provided strong evidence supporting translocation of the RCL during the transition of the Michaelis complex to covalent acyl−enzyme complex. It is still unclear whether insertion of the reactive center loop into β-sheet A requires single or multiple structural transitions in the serpin tertiary structure.

† This work was supported by the National Institutes of Health Grant HL 54930 (to J.D.S.).

* To whom correspondence should be addressed. Tel: (313) 876-7228. FAX: (313) 876-2380. E-mail:jshore1@hfhs.org.

‡ Henry Ford Health Sciences Center.

§ Wayne State University School of Medicine.

10.1021/bi025967p CCC: $22.00
Published on Web 09/13/2002

Methodologies for probing structure/function relationships and conformational changes of proteins often involve site-directed mutagenesis and/or residue specific labeling with fluorescent probes (*4*, *13*, *14*, *20*, *21*). The limitation of these approaches is that they require alterations of the protein, which may affect function and/or monitor conformational changes at the specific site of fluorescent probe attachment. An alternative method is the biosynthetic incorporation of non-natural amino acid analogues with altered spectral properties for characterization of protein conformational changes (*22*−*26*). Tryptophan residues have commonly been utilized as a sensitive intrinsic fluorescent probe for monitoring the dynamics of conformational change. However, the use of intrinsic tryptophan fluorescence when investigating protein−protein interactions is difficult to interpret due to fluorescence contributions of both proteins (*27*). Tryptophan analogues provide a new basis for studying conformational changes of a protein due to their interactions with other tryptophan containing proteins because of the red-shifted absorbance shoulder of the analogue allowing specific fluorescence excitation. A number of investigators have studied a series of synthetic tryptophan analogues with a varying range of chemical and photophysical properties (*22*, *24*, *28*).

Using plasminogen activator inhibitor-1 (PAI-1) as a paradigm for serpins, we have used the biosynthetic incorporation of 7-azatryptophan (7-ATrp) to develop a species in which we can follow overall structural transitions. The advantages of using PAI-1 as a model serpin in this study over other serpins are severalfold. It contains two other tryptophan residues in addition to the two that are highly conserved in the serpin fold (*1*). All four residues are located in regions of the molecule that would likely be inaccessible to fluorescent probe labeling and are located near regions believed to be mobile and directly involved in serpin function. Thus, the combined fluorescence of these tryptophan residues can report overall changes in the molecular structure without the limitations of a single tethered fluorescent probe. The four Trp residues, 86, 139, 175, and 262 (PAI-1 numbering), are near the mobile β-strands 1A and 2A (*3*), on α-helix F, in the conserved serpin breach region at the point where the RCL first inserts, and on α-helix H near the C-terminal cleavage fragment, respectively (Figure 1) (*14*, *29*−*33*). Figure 1 illustrates the changes of overall structure and position of the tryptophan residues in PAI-1 prior to and following cleavage of the RCL and the associated stressed to relaxed transition (*30*, *33*). In addition to the red-shifted absorbance, 7-ATrp shows high sensitivity to changes in microenvironment and is quenched by water, making it a highly useful probe for following protein conformational changes (*22*). The incorporation of 7-ATrp into proteins, in effect, only replaces the C-7 carbon of the Trp indole ring with a nitrogen, resulting in a protein in which the Trp residues have similar van der Waals radii but an increase in polarity and electron density around the N-7 nitrogen that would permit the evaluation of local molecular interactions (Figure 2) (*28*, *34*, *35*).

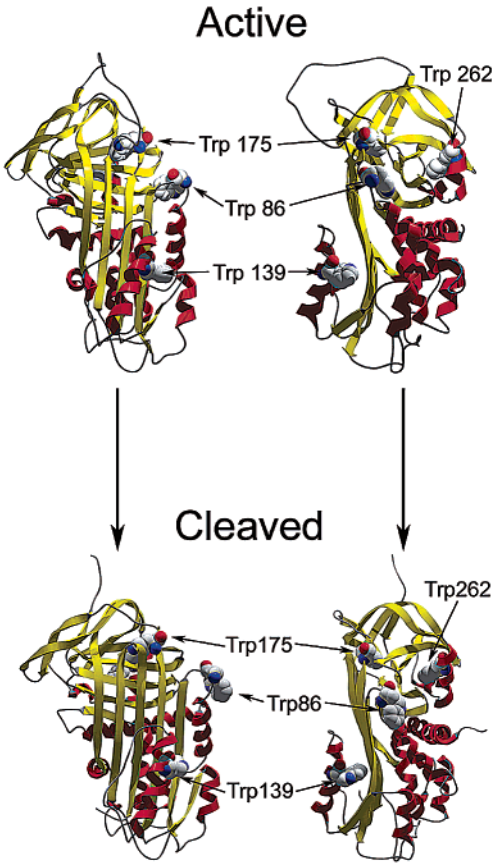

FIGURE 1: Illustration of the structural changes and localization of the tryptophan residues in PAI-1 following the stressed to relaxed transition. The active (stressed) and cleaved (relaxed) structures of PAI-1 are each depicted in two views with the same orientations. The positions of tryptophan residues are indicated. The β-sheet structures are indicated in yellow, α-helices are indicated in red, and tryptophan residues are represented as cpk-colored space-filled models. The figure was generated in Swiss PDB Viewer (ver. 3.72b), using the coordinates for active PAI-1 (PDB code 1B3K, chain A in ref *30*) and cleaved PAI-1 (PDB code 9PAI, ref *33*).

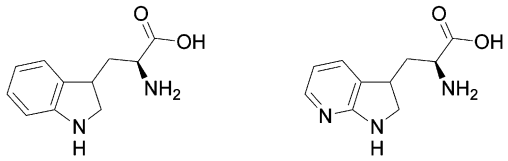

FIGURE 2: Tryptophan and 7-azatryptophan chemical structures. Chemical structures were generated using the program CS ChemDraw Ultra (ver. 6.0).

By using 7-ATrp as an intrinsic fluorescence probe, we have directly observed the conformational changes during the serpin inhibition mechanism, demonstrating a molecular rearrangement of the serpin structure concomitant with inhibition of a proteinase. Here we report fluorescence and rapid kinetic studies for PAI-1 inhibition of its two physiological target proteinases, t-PA and u-PA, that indicate a concerted molecular rearrangement of β-sheet A, the F-helix,

[1] Abbreviations: PAI-1, plasminogen activator inhibitor type 1; 7-ATrp PAI-1, 7-azatryptophan incorporated wtPAI-1; α_1ACH, α_1-antichymotrypsin; RCL, reactive center loop; t-PA, tissue type plasminogen activator; (S195A)t-PA, Ser → Ala active-site mutant of tissue type plasminogen activator; u-PA, urokinase plasminogen activator; PCR, polymerase chain reaction; SDS-PAGE, sodium dodecyl sulfate polyacrylamide gel electrophoresis; 7-ATrp, 7-azatryptophan; 5-OHTrp, 5-(hydroxy)tryptophan; F-Trp, 4-, 5-, or 6-fluorotryptophan; HEPES, 4-(2-hydroxyethyl)piperazine-1-ethansulfonic acid; EDTA, ethylenediame-tetraacetic acid; NBD, *N*,*N*′di-methyl-*N*-(acetyl)-*N*′-methyl(7-nitrobenz-2-oxa-1,3-diazol-4-yl)ethylenediamine; MSA, methanesulfonic acid.

and the breach region that coincides with RCL insertion and proteinase trapping without any prior conformational changes due to formation of the noncovalent Michaelis complex. In addition, we observed a reduction in the rate of conformational change and inhibitory efficiency of 7-ATrp PAI-1 against t-PA but not u-PA, demonstrating sensitivity of the PAI-1 structure to localized atom level mutations in the Trp residues that are target-proteinase-specific.

EXPERIMENTAL PROCEDURES

Materials. Unless otherwise indicated, all spectral and kinetic measurements were performed at pH 7.4 and 25 °C in a reaction buffer with an ionic strength of 0.15 and containing 30 mM HEPES, 0.135 M NaCl, 1 mM EDTA. Acrylic sample cuvettes were coated with 0.1% poly(ethylene glycol) for reduction of protein adsorption. Spectozyme^{tPA} (CH_3SO_2-D-HHT-Gly-Arg-*p*NA) and Spectrozyme^{UK} (Cbo-L-(γ)Glu(a-t-BuO)-Gly-Arg-*p*NA) were from American Diagnostica Inc. (Greenwich, CT). Chromatography materials and the ECL+Plus Western Blotting detection kit were from Amersham Pharmacia Biotech (Uppsala, Sweden). Pancreatic elastase and DL-7-azatryptophan were from Sigma, and L-tryptophan was from Fisher Biotech. Restriction enzymes were from Promega. Oligonucleotides were synthesized and provided HPLC purified by Cruachem. Methanesulfonic acid was obtained from Fluka Biochemika. All other reagents were of analytical reagent grade or better and obtained from Sigma or Fisher Biotech. Rabbit polyclonal anti-human PAI-1 antibody was obtained from Molecular Innovations, Inc., and anti-rabbit IgG-HRP conjugate was from Santa Cruz Biotechnology, Inc.

PAI-1 Variants and t-PA Protein. Recombinant human PAI-1 was a generous gift from Dr. David Ginsburg (Howard Hughes Medical Institute, Ann Arbor, MI) and provided as a clone without the signal peptide in the vector pET-3a. The PAI-1 insert was amplified by PCR using the forward and reverse primers 5′-GGTTTCCCTCTAGAATTCATTTTGTTTAACTT-3′ and 5′-GTGGCAGCAGCCAACTAAGCTTCCTTTCGGGC-3′ to introduce EcoRI and HindIII restriction sites, respectively. The amplified PAI-1 was subsequently restriction cut with EcoRI and HindIII and ligated into pET-24d (Novagen). For expression in *Escherichia coli*, PAI-1 was transformed into the host BL21(DE3) pLysS (Novagen) and cultured in LB media to an OD_{600} of 0.3−0.5 prior to induction of protein expression for 2 h by the addition of IPTG to a final concentration of 1 mM. Bacterial lysates were obtained by the lysozyme-freeze/thaw method of Sambrook et al. (*36*). The soluble active and latent PAI-1 fractions were purified and separated by heparin-, phenyl-, and SP-substituted sepharose chromatography as previously described (*37*). Biosynthetic incorporation of 7-ATrp into PAI-1 required the use of an auxotrophic strain of *Escherichia coli*, W3110*TrpA88*(DE3), provided by Dr. Thomas Heyduk at St. Louis University Medical School and modified such that the tryptophan operon is deleted (*22*). The host strain was further modified by the introduction of the pLysS plasmid (Novagen) containing the gene for T7 lysozyme, a repressor to the T7 promoter, to reduce background expression prior to analogue supplementation. We utilized the one-step method for incorporation of 7-ATrp as described by Ross (*22*) with the following modifications. In brief, host cells containing PAI-1 pET-24d constructs are cultured in M9 minimal media (*36*) supplemented per liter with 2% casamino acids, 0.01% thiamin, 2 mM $MgSO_4$, 0.4% glucose, 0.4% glycerol, 0.1 mM $CaCl_2$, and 0.02 mM L-Trp. Cells reached a limiting density after ∼16 h of incubation at 37 °C and consumption of all available L-Trp (∼OD_{600} 0.8−1.0), after which DL-7-ATrp was added to a final concentration of 0.5 mM. Following a 10 min incubation in the presence of 7-ATrp, protein expression was induced by IPTG for 2−3 h, and cell lysates were harvested as described above. PAI-1 protein concentrations were measured at 280 nm, using an extinction coefficient of 0.93 mL mg^{-1} cm^{-1} and a M_r of 43 000 (*37*−*38*) or by the Bradford dye-binding assay (Bio-Rad) using purified wtPAI-1 as a standard (*39*).

Human recombinant t-PA (Activase) and the (S195A)t-PA, the active-site (Ser → Ala) mutant at residue 195 was kindly provided by Genentech Inc. (San Francisco, CA). The predominantly single chain t-PA was converted to the two-chain form by treatment with immobilized plasmin as previously described (*7*). Human recombinant high molecular weight u-PA was provided by Abbott Laboratories (Chicago, IL).

Western Blot Analysis of PAI-1 Background Expression. Background protein expression was quantified by comparing PAI-1 expression before and after induction. Duplicate expression cultures were prepared essentially as described above in 0.5 L volumes. Prior to induction, one culture was harvested and stored at 4 °C, while the other was supplemented with 7-ATrp and induced for an additional 3 h with IPTG. The total protein in bacterial lysates was normalized to an A_{280} of 0.7 for both the pre- and post-induction samples and diluted in standard HEPES buffer to a concentration of 23 μg/mL using an extinction coefficient of 1.0 at 280 nm and then mixed 3:1 with 4× concentrated SDS-PAGE loading buffer (17.3 μg/mL final concentration). Samples of 15 μL were resolved by 10% SDS-PAGE under reducing conditions on duplicate gels and either stained or transferred to PVDF membranes. Western blots were developed by first blocking in 0.038 M Na_2HPO_4, 0.011 M NaH_2PO_4, 0.145 M NaCl, 0.5% Tween-20, 1.0% Triton X-100, pH 7.5 (PBS-T), containing 5% milk w/v for 60 min. The blot was reacted with 1.2 mg/mL anti-PAI-1 polyclonal Ab (1:10,000) in PBS-T containing 5% milk for 60 min, followed by two washes in PBS-T, and then incubation with anti-rabbit IgG-HRP conjugate (1:10,000) for another 60 min. After three washes in PBS-T, the blot was developed using the ECL+Plus chemiluminescence detection kit per manufacturer's instructions and Kodak BioMax-ML film. Analysis of the immunoblot bands were performed on a Gel Doc Imaging system and quantified using the Quantity One software package (Bio-Rad).

Analysis of Analogue Incorporation Efficiency. The procedure to determine analogue incorporation was based on a methodology under development and information provided by Glenn Abbott (in the laboratory of A. G. Szabo, Department of Chemistry, Wilfrid Laurier University, Waterloo, Ontario) (personal communcation). Amino acid hydrolysis using methanesulfonic acid (MSA) (*40*) and analysis of the aromatic residues by analytical reverse phase HPLC were used to determine analogue incorporation. A total of 2.9 mg of 7-ATrp PAI-1 was dialyzed into 0.3 M ammonium acetate pH 6.0 (NH_4OAc), snap frozen in liquid N_2, and lyophilized. The lyophilized protein was resuspended in 200 μL of milliQ

H_2O, transferred into an 8 mm × 60 mm vacuum hydrolysis tube, and mixed with 40 μL of 4 M MSA. Hydrolysis was carried out for 24 h at 115 °C and the reaction quenched with 44 μL of 4 M KOH prior to being snap frozen in liquid N_2 and lyophilized.

Analytical HPLC was carried out on a Waters model 600/600E pump and controller system connected to a model 991 photodiode array detector set to monitor UV absorbance between 200 and 400 nm. The hydrolyzate was resuspended in 100 μL of 0.15 M NH_4OAc, pH 6.0, and 20 μL was mixed with either 10 μL of 0.15 M NH_4OAc or 10 μL of known concentrations of Trp and 7-ATrp standards diluted in 0.15 M NH_4OAc, followed by injection onto a Beckman Ultrasphere C-18 reverse phase column (5 μm, 0.46 cm × 25 cm i.d.) using a 20 μL sample injection loop. Aromatic amino acids were separated essentially as described (*41*) using a 1.0 mL/min flow rate and a 30 min linear gradient from 100% solvent A (0.07 M sodium acetate, 5% methanol and 0.25 mL/L triethylamine, pH 4.5) to 100% solvent B (methanol). Concentrations of Trp and 7-ATrp in the hydrolyzate were determined by internal standard addition. The integrated absorbance of Trp and 7-ATrp elution peaks at 280 and 295 nm were plotted against the concentrations of the internal standards and fitted by linear regression. Relative concentrations of Trp and 7-ATrp were calculated using the slopes of the linear regressions from the standard addition and the integrated absorbance of Trp and 7-ATrp elution peaks in the absence of added standard. To confirm that MSA does not degrade Trp or 7-ATrp during the amino acid hydrolysis reaction, 0.8 μmol of Trp and 7-ATrp free acid standards was subjected to identical hydrolysis conditions as used for 7-ATrp PAI-1, with and without the addition of 4 M MSA. Reverse-phase HPLC analysis indicated that 100% of the Trp and 99.1% of the 7-ATrp was recovered under our hydrolysis conditions (data not shown).

Peptide-Blocked Substrate PAI-1. The complex of 7-ATrp PAI-1 and Ac-TVASSSTA, which functions as a substrate for t-PA, was prepared essentially as described (*7*). In brief, peptide-blocked PAI-1 was prepared by mixing 0.5 mL of 20 μM 7-ATrp PAI-1 in 5 mM NaPi, 0.345 M NaCl, and 1 mM EDTA (pH 6.2) with 0.5 mL of 2 mM Ac-TVASSSTA contained in standard HEPES buffer for 260 h at 25 °C. Formation of octapeptide-blocked species was monitored over time by reacting 10 μL samples with excess t-PA and resolution on 10% SDS-PAGE. The final product was determined to be greater than 95% substrate and subsequently desalted on a 5 mL HiTrap G-25 column (Pharmacia) to remove excess peptide.

Circular Dichroism Spectroscopy. Far- and near-UV CD spectra were measured with an Aviv 60DS Circular Dichroism Spectrometer with a peltier controlled cell holder and running IGOR Pro 3.02 software (Wavemetrics). Protein concentrations of active and latent wtPAI-1 or 7-ATrp PAI-1 were from 8 to 10 μM to yield an A_{220} of 0.8 in a buffer containing 50 mM NaPi and 0.15 M NaF adjusted to pH 6.6. Spectra were subsequently normalized by protein concentration. Far and near-UV CD spectra were obtained by scanning from 260 to 195 nm or 320 to 250 nm using 2 or 5 mm cuvettes, respectively. All spectra are reported as a three-scan average with a 15 s integration over a 1 nm step resolution.

Functional Inhibitor Concentration and SDS-PAGE Analysis of the Substrate Pathway. The stoichiometry of inhibition (S.I.), defined as the number of moles of inhibitor required to inhibit one mole of proteinase, was determined from residual proteinase activity following reaction with wtPAI-1 or 7-ATrp PAI-1. Reactions containing 200 nM t-PA or u-PA were preincubated in a 100 μL volume of 30 mM HEPES, 0.135 M NaCl, 1 mM EDTA, 0.1% PEG, pH 7.4, with 0−1.8-fold concentrations of wtPAI-1 or 7-ATrp PAI-1 for 60 min at 25 °C. Reactions were subsequently diluted into 1 mL of reaction buffer containing 0.1 mM of the appropriate chromogenic substrate (Spectrozyme^{tPA} or Spectrozyme^{UK}) and initial reaction rates monitored at 405 nm. Residual proteinase activity was plotted versus the molar ratio of PAI/proteinase, and the S.I. was calculated from the extrapolated *x*-intercept of the best-fit linear regression to the data. S.I. determinations were repeated at least twice and are reported as averages of replicate experiments ± S.E.M.

SDS-PAGE analysis of wtPAI-1 or 7-ATrp PAI-1 (2 μM) reactions were carried out following incubation at 25 °C in reaction buffer for 15 min with t-PA (4 μM) or u-PA (4 μM). Reactions were quenched with 18.75 μL of 0.2 M HCl, followed by concentrated electrophoresis buffer to a final concentration of 1% SDS. Typically 30−40 μL of the quenched reactions were resolved by 10% SDS-PAGE, stained, and digitized for band density analysis as described elsewhere (*7*). Band densities for unreactive (latent) and cleaved PAI-1 were quantitated as described (*7*) and compared to those of parallel reactions in the absence of t-PA or u-PA. Data are reported as averages of at least three independent experiments ± S.E.M.

Apparent Second-Order Rate Constants for Binding of PAI-1 and 7-ATrp PAI-1 to t-PA. The apparent bimolecular rate constants, k_{app}, for the irreversible inhibition of t-PA or u-PA by wtPAI-1 and 7-ATrp PAI-1 were determined by the competitive kinetic method (*42*) with the chromogenic substrates Spectrozyme^{tPA} and Spectrozyme^{UK} (0.5 mM). The procedure is described elsewhere (*7*, *19*) with the following concentrations used for wtPAI-1 (100 nM) or 7-ATrp PAI-1 (100−250 nM) and t-PA or u-PA (10−20 nM). Inhibition progress curves were monitored at 405 nm and were fit by a single-exponential function with a linear component to obtain the pseudo-first-order rate constant, k_{obs}. The second-order bimolecular rate constant was obtained by dividing k_{obs} by the functional inhibitor concentration (i.e., inhibitor concentration divided by the S.I., *43*) and then multiplying by the factor $1 + [S_0]/K_M$ to correct for the competitive effect of the substrate in the serpin−proteinase reaction. Data are reported as averages of at least three independent experiments ± S.E.M.

Fluorescence Spectroscopy and Stopped-Flow. Fluorescence measurements were recorded on a SLM 8000 Spectrofluorimeter. The excitation wavelength used for studying the fluorescence of 7-ATrp PAI-1 was 315 nm and the emission spectra were scanned from 325 to 425 nm. The excitation wavelength for wtPAI-1 was 295 nm, and the emission was scanned from 310 to 460 nm. For assays of PAI-1•t-PA covalent complex formation, 7-ATrp PAI-1 (0.5 μM) was reacted with t-PA or (S195A)t-PA (1.0 μM) in reaction buffer for 10 min to ensure a complete reaction prior to initiating the emission scan. For reactions with elastase, 7-ATrp PAI-1 (0.5 μM) was incubated for 25 min in the

presence of elastase (0.1 μM) prior to recording emission data. Octapeptide-blocked 7-ATrp PAI-1 (0.5 μM) spectra were recorded before and after insertion of Ac-TVASSSTA. All emission scans are averages of three independent data collections with a 5 s integration over a 1 nm step resolution.

For assays of spontaneous inactivation, 7-ATrp PAI-1 (0.5−1.0 μM) and wtPAI-1 (0.5 μM) were incubated at 25 °C in reaction buffer with emission spectra collected at various time points. The data were normalized using the relationship $(F - F_o)/F_o$, where F is the total fluorescence of the emission peak at each time interval and F_o is the initial fluorescence emission. Normalized data were analyzed by nonlinear least-squares fitting to the function of a first-order reaction to obtain k_{obs}. The half-life for spontaneous inactivation is described by the equation $\ln 2/k_{obs} = t_{1/2}$. Data are reported as averages of at least three independent experiments ± S.E.M.

Stopped-flow fluorimetry was measured on an Applied Photophysics SX.18MV Stopped-Flow Reaction Analyzer with a thermostated syringe chamber. Excitation was at 315 nm, and a filter with a cutoff below 335 nm was used to monitor fluorescence emission. Stopped-flow experiments were carried out as previously described under pseudo-first-order conditions with t-PA or u-PA in excess over 7-ATrp PAI-1 (0.125−0.25 μM) (*4*). The value for k_{obs} was obtained by fitting the fluorescence change in the stopped-flow traces to a single-exponential decay function. The data were analyzed assuming the two-step binding mechanism of serpin inhibition (*44*) for which the dependence of k_{obs} on proteinase concentration is described by the function for a rectangular hyperbola

$$k_{obs} = \frac{k_{lim} \times [E]_o}{K_M + [E]_o}$$

where [E] is the proteinase concentration, k_{lim} represents the apparent 1st order rate constant for the formation of an inhibited serpin−proteinase complex, and K_M is the concentration of proteinase at which k_{obs} reaches one-half of k_{lim} and is given by $(k_{-1}+k_2)/k_1$, where k_1 and k_{-1} are the forward and reverse rate constants for formation of the noncovalent Michaelis complex, respectively (*4*, *14*, *44*).

SDS-PAGE Analysis of Spontaneous Inactivation. Wild-type PAI-1 and 7-ATrp PAI-1 (4 μM) were incubated at 25 °C in parallel. At the various time points, 25 μL aliquots were removed and mixed with 25 μL of t-PA (8 μM) to yield final reaction concentrations of 2 and 4 μM, respectively. Following a 15 min incubation, reactions were quenched with 18.75 μL of 0.2 M HCl, followed by concentrated electrophoresis buffer to a final concentration of 1% SDS. Typically 30−40 μL of the quenched reactions were resolved by 10% SDS-PAGE, stained, and digitized for band density analysis as described elsewhere (*7*). Reaction product band densities were analyzed by nonlinear least-squares fitting to the function of a first-order decay reaction to obtain k_{obs}, and $t_{1/2}$ was determined as described above.

Limiting Rate Constant for the Formation of the Inhibited Serpin−Proteinase Complex. The rate of formation of the inhibited serpin−proteinase complex of t-PA and 7-ATrp PAI-1 was determined using the rapid acid quenching technique. Reactions containing 7-ATrp PAI-1 (2.0 μM) and t-PA (1.0 μM) were reacted for various times in an aging loop prior to quenching with 0.2 M HCl to a final pH of 2.0, neutralization with 1.0 M NaOH, and resolution by 10% SDS-PAGE. Acid quenching to pH 2.0 protonates the His57 residue of the serine proteinase catalytic triad, freezing the reaction (*7*). Electrophoresis gels were stained with Gelcode (Pierce), and digital images of the trans-illuminated gels were recorded in the dark using a CCD camera (Bio-Rad GelDoc). The rapid acid quenching technique and analysis of the reaction products (PAI-1•t-PA complex and RCL cleaved PAI-1) from digitized SDS-PAGE gels is described elsewhere (*7*). To obtain the k_{lim} value for formation of the inhibited complex, reaction progress curves were analyzed by nonlinear least-squares fitting to the function of a first-order reaction and reported as averages of at least three independent experiments ± S.E.M.

RESULTS

Biosynthetic Incorporation of 7-ATrp into PAI-1. A suitable approach for incorporation of non-natural amino acids is through recombinant protein expression in an auxotrophic strain of *E. coli*. To determine whether 7-ATrp analogue incorporation affects protein expression, expressions supplemented with L-Trp or DL-7-ATrp were compared by 10% SDS-PAGE and western transfer, followed by immunoblot analysis with polyclonal rabbit anti-PAI-1. As previously observed with other proteins (*22*), soluble PAI-1 expression in the presence of DL-7-ATrp was reduced compared to that observed when the media were supplemented with L-Trp (data not shown). The efficiency of 7-ATrp analogue substitution was quantified by subjecting 7-ATrp PAI-1 protein to acid hydrolysis with MSA, which does not degrade Trp residues (*40*), and then separating the aromatic residues by analytical reverse phase HPLC (*41*). Retention times for 7-ATrp (11.46 ± 0.06 min) and Trp (15.09 ± 0.13 min) from 7-ATrp PAI-1 hydrolyzates were consistent with free acid standards and previous observations (*41*)(Figure 3).

Quantitative analysis indicated that the 7-ATrp PAI-1 preparation was 73.7% substituted with 7-ATrp. It has been reported that decreased analogue incorporation efficiency can be attributed to "leaky" promoters (*22*), and it is possible that the presence of native Trp in the 7-ATrp PAI-1 preparation was due to wtPAI-1 molecules that arose from background protein expression. We measured the background wtPAI-1 expression by comparing expression levels in the auxotrophic *E. coli* strain before and after induction. Pre- and post-induction samples were compared by 10% SDS-PAGE and western transfer (Figure 4A,B). Quantitative immunoblot analysis indicated that only 2.5% of the total PAI-1 protein was expressed prior to supplementation with 7-ATrp and IPTG induction. Thus, native Trp incorporated into 7-ATrp PAI-1 could likely be attributable to residual endogenous Trp present in the *E. coli* before IPTG induction and protein turnover post-IPTG induction. This would lead to a random distribution of native Trp incorporation among the four residue positions. A variable tolerance for 7-ATrp substitutions at specific Trp positions would lead to a non-random distribution of the residual native Trp. Despite the fractional Trp presence, incorporation of 7-ATrp into PAI-1 produced a red-shifted absorbance spectrum that permitted specific excitation at 315 nm, a wavelength at which natural Trp does not absorb (*22*). Thus, residues replaced

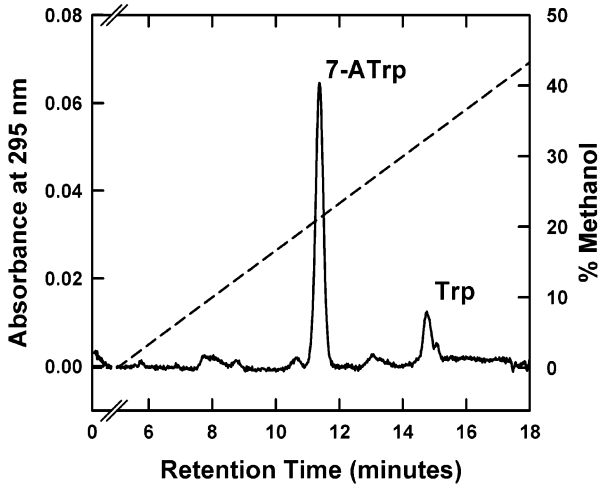

FIGURE 3: Reverse-phase HPLC of the 7-ATrp PAI-1 hydrolyzate. Elution of amino acids following hydrolysis of 7-ATrp PAI-1 with MSA for 24 h at 115 °C was performed on a C-18 RP column using a linear gradient of 0.07 M sodium acetate, 5% methanol, and 0.25 mL/L triethylamine, pH 4.5, to 100% methanol as described in Experimental Procedures. Sample volumes of 20 μL were injected and the amino acids detected using a photodiode array detector (200 nm-400 nm). The represented elution profile at 295 nm indicates the retention times of Trp and 7-ATrp in the absence of added free acid standards. The absorbance of Tyr and Phe is undetectable at 295 nm. The dashed line represents the linear gradient profile.

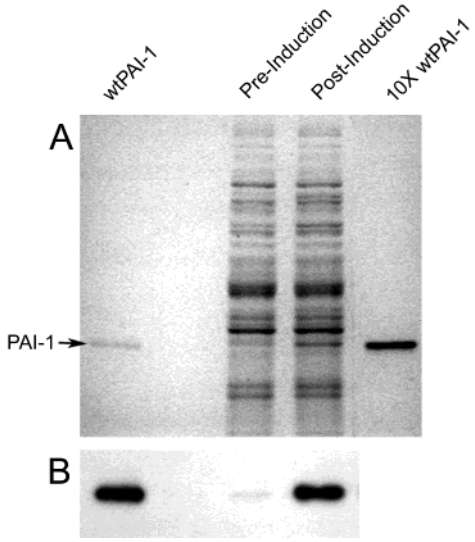

FIGURE 4: SDS-PAGE and Western blot analysis of pre-induction wtPAI-1 expression. Background wtPAI-1 protein expression was quantified by comparing 7-ATrp PAI-1 expressions before and after induction as described in Experimental Procedures. Panel A: A total of 15 μL of each sample was resolved by 10% SDS-PAGE, wtPAI-1 (2.5 μg/mL), lane 1; pre-induction lysate (17.3 μg/mL), lane 2; post-induction lysate (17.3 μg/mL), lane 3; 10x wtPAI-1 (25 μg/mL), lane 4. Panel B: Western blot analysis of the duplicate gel to that shown in panel A, wtPAI-1 (2.5 μg/mL), lane 1; pre-induction lysate (17.3 μg/mL), lane 2; post-induction lysate (17.3 μg/mL), lane 3. The 10x wtPAI-1 lane is not shown due to the over-exposure on the blot. Band density analysis is described in the text.

by 7-ATrp are specifically excited without exciting Trp residues on other proteins such as t-PA or PAI-1 (Figure 5).

Biochemical Characterization of 7-ATrp PAI-1. For any approach that utilizes a mutant or altered form of the protein, it is important to determine if the structural integrity is

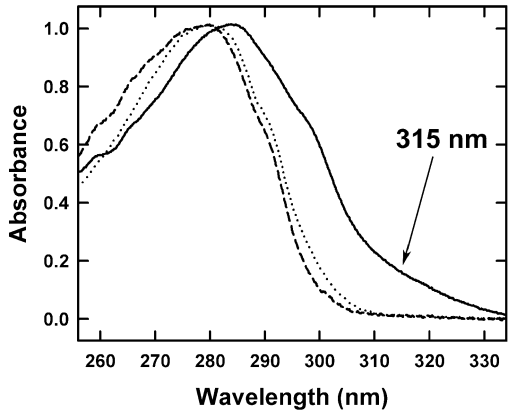

FIGURE 5: Absorbance spectra of wtPAI-1, 7-ATrp PAI-1, and t-PA. Absorbance spectra were recorded at a concentration of 10 μM in standard HEPES buffer. Spectra were subsequently normalized to an absorbance of 1.0. The arrow indicates the excitation wavelength at 315 nm for 7-ATrp PAI-1. 7-ATrp PAI-1, solid line; wtPAI-1, dashed line; t-PA, dotted line.

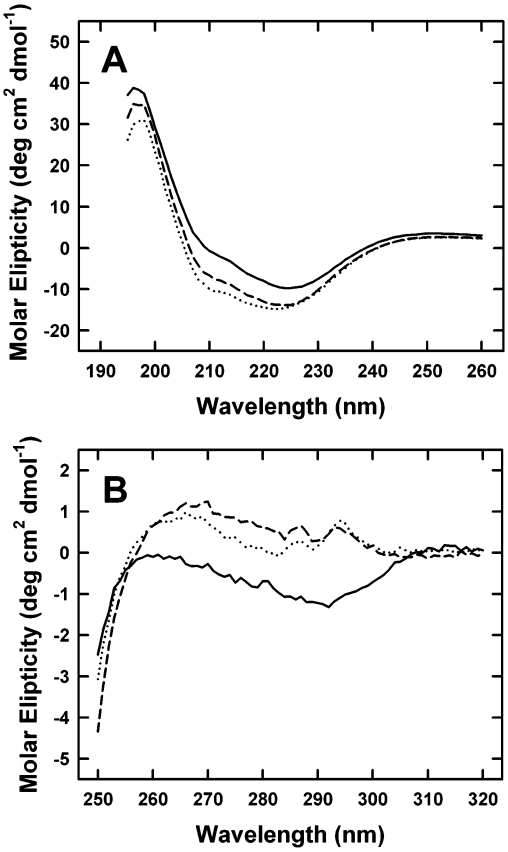

FIGURE 6: Far and near-UV circular dichroism spectra of 7-ATrp PAI-1 and wtPAI-1. Far and Near-UV CD profiles were recorded at a concentration of 8−10 μM and 25 °C as described in Experimental Procedures. Panel A: Far-UV CD, 7-ATrp PAI-1, solid line; wtPAI-1, dashed line; latent wtPAI-1, dotted line. Panel B: Near-UV CD, 7-ATrp PAI-1, solid line; wtPAI-1, dashed line; latent wtPAI-1, dotted line.

compromised following analogue incorporation. For this purpose we collected far and near-UV CD spectra of active 7-ATrp PAI-1 compared with those of active and latent wtPAI-1 controls at 25 °C. The far-UV CD spectra of active and latent wtPAI-1 are aligned with 7-ATrp PAI-1 and shown in Figure 6A. As previously observed, both active and latent wtPAI-1 had comparable far-UV CD profiles indicating minimal changes in overall secondary structure in response

Table 1: Kinetic Parameters for 7-ATrp PAI-1 and WtPAI-1[a]

	t-PA			u-PA			
PAI-1	k_{app} (μM^{-1} s^{-1})	S.I. (mol I/mol E)	cleaved (%)	k_{app} (μM^{-1} s^{-1})	S.I. (mol I/mol E)	cleaved (%)	$t_{1/2}$ of latency[b] (hr)
wtPAI-1	15.4 ± 1.4	1.2 ± 0.01	6.4 ± 1.3	8.1 ± 0.7	1.2 ± 0.1	5.6 ± 1.2	13.6 ± 2.8 (17.8 ± 2.4)
7-ATrp PAI-1	3.3 ± 0.2	1.2 ± 0.01	11.8 ± 0.4	8.4 ± 0.7	1.4 ± 0.1	10.2 ± 0.6	36.9 ± 1.2 (29.6 ± 1.7)

[a] Kinetic parameters were determined in 0.03 M HEPES/0.135 M NaCl/1 mM EDTA at pH 7.4 and 25 °C. All data are reported as averages of at least three independent experiments ± S.E.M. [b] Values are taken from experiments following the active to latent transition with fluorescence. Those in parentheses are calculated from experiments monitoring loss of inhibitory activity.

to the active to latent transition and RCL insertion (*45*). A similar CD profile was observed with 7-ATrp PAI-1, suggesting that analogue incorporation does not significantly alter PAI-1 secondary structures. The small deviations between the wtPAI-1 and 7-ATrp PAI-1 spectra could reflect spectral properties of the 7-ATrp probe since far-UV CD spectra has been shown to be sensitive to aromatic side chains (*46*). The near-UV CD, which is mainly attributed to the three aromatic residues Trp, Tyr, and Phe, showed an expected difference in mean residue elipticity in the region of 260−300 nm, consistent with alterations of the local Trp environments upon probe incorporation (Figure 6B).

Although there was no overall effect on the structural fold of 7-ATrp PAI-1, replacement of Trp residues with 7-ATrp did affect the inhibitory function of PAI-1 by reducing the apparent second-order rate constant (k_{app}) for t-PA inhibition by 7-ATrp PAI-1 (Table 1). Consistent with our previous observations (*4*, *7*), the k_{app} of the wtPAI-1 control was determined to be 15.4 ± 1.4 μM^{-1} s^{-1}, whereas the k_{app} for 7-ATrp PAI-1 was reduced to 3.3 ± 0.2 μM^{-1} s^{-1}. In contrast, inhibition of u-PA by 7-ATrp PAI-1 was not affected by the analogue incorporation and was consistent with wtPAI-1 controls (Table 1). Single-point mutations that affect the inhibitory activity of PAI-1 toward t-PA but not u-PA have been observed (*20*,*47*, *48*), but often primarily resulted in the cleavage of PAI-1 as a substrate by t-PA but not u-PA (*48*). Despite the decrease in the inhibitory efficiency of PAI-1 upon incorporation with the 7-ATrp, we did not observe any significant effects on the S.I. compared to that of wtPAI-1 controls (Table 1). The S.I. values are greater than the theoretical 1.0 expected for a 1:1 complex of serpin and proteinase due to the bifurcating pathway with one branch leading to covalent complex and the other to cleaved serpin (*43*, *49*). To further investigate the relative amount of cleaved PAI-1 formed in the reaction with t-PA or u-PA, wtPAI-1 and 7-ATrp PAI-1 were reacted with a 2-fold molar excess of t-PA or u-PA for 15 min to ensure complete reaction and subsequently analyzed by SDS-PAGE and band density analysis. 7-ATrp PAI-1 indicated an increased amount of hydrolyzed PAI-1 (11.8 ± 0.4%) compared to that of wtPAI-1 with only 6.4 ± 1.3% of the PAI-1 being hydrolyzed and not trapped in an acyl−enzyme complex with t-PA (Table 1). The amount of 7-ATrp PAI-1 cleaved by u-PA was comparable to experiments with t-PA (Table 1).

Conformational Changes in PAI-1 Observed by 7-ATrp Fluorescence. To determine whether conformational changes in PAI-1 could be detected by 7-ATrp as an intrinsic fluorescence probe, emission spectra in the absence and presence of a 2-fold molar excess of t-PA were recorded.

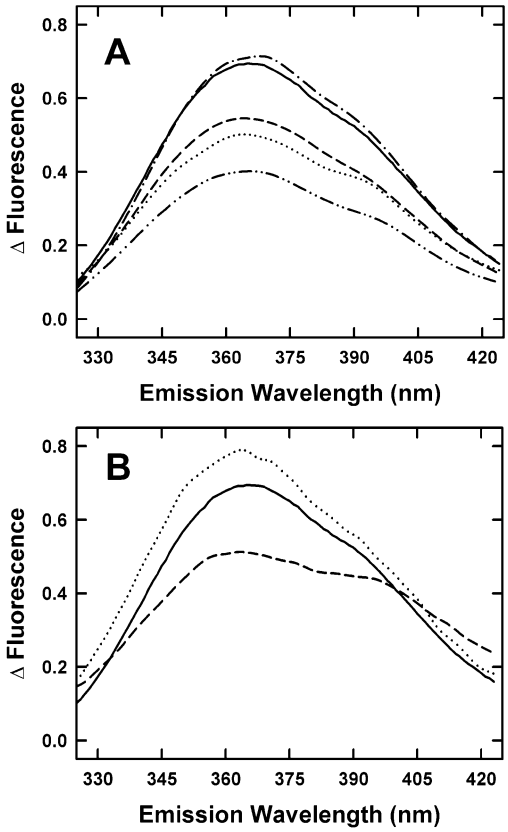

FIGURE 7: Altered fluorescence of 7-ATrp PAI-1 due to local conformational changes. Panel A: Fluorescence emission spectra (excitation at 315 nm) of 7-ATrp PAI-1 (0.5 μM) were recorded in the absence of (solid line) or following reaction with elastase (0.1 μM) (dashed line), t-PA (1.0 μM) (dotted line), or (S195A)t-PA (dashed−dotted−dashed line), as described in Experimental Procedures. Emission spectra of latent PAI-1, dashed−dotted−dotted−dashed line. Panel B: Fluorescence emission spectra (excitation at 315 nm) were recorded prior to the addition of Ac-TVASSSTA octapeptide (2 mM) (solid line), directly following octapeptide addition (t = 0) (dotted line), and after complete insertion as strand s4A of β-sheet A (dashed line). Insertion of octapeptide Ac-TVASSSTA is described in Experimental Procedures. All emission profiles are averages of three independent experiments. Relative percent changes in fluorescence are described in the text and reported as an averaged value ± S.E.M.

Reaction of 7-ATrp PAI-1 with t-PA and formation of the acyl−enzyme complex resulted in a 26.1 ± 3.3% quench of fluorescence with a broad peak at 364 nm, slightly blue-shifted from the peak observed for active 7-ATrp PAI-1 at 366 nm (Figure 7A).

Since there are no Trp residues directly on the RCL, the observed fluorescence change upon proteinase binding reflects either environmental shifts localized near individual

Trp residues or direct spectral perturbation by the proteinase. To determine if the change is due to loop cleavage and insertion, emission spectra were recorded before and after reaction with catalytic amounts of elastase. Elastase cleaves PAI-1 at the P3−P4 peptide bond of the RCL permitting loop insertion without formation of a covalent acyl−enzyme complex (*50*). The resulting PAI-1 species serves as a conformational model with the cleaved RCL inserted as strand s4A of β-sheet A. As shown in Figure 7A, cleavage by elastase demonstrated a similar quench in fluorescence of 20.5 ± 1.6% and an identical blue shift to 364 nm, consistent with the fluorescence quench representing conformational changes occurring due to insertion of the RCL. These data also indicate that the trapped proteinase has little effect on the local environments of 7-ATrp residues since the fluorescence change is almost entirely dependent upon structural changes in PAI-1.

Studies using α_1-antichymotrypsin (α_1ACH) as a model serpin have proposed that prior to loop cleavage and insertion, there are sequential rearrangements in the RCL and a two-step mechanism to facilitate full loop insertion into β-sheet A (*18*, *51*). The authors have suggested that residues P14 through P12 partially insert into β-sheet A, breaking stabilizing hydrogen bonds, and that there is an introduction of the α-helix F/s3A turn into the crevice between strands s3A and s5A to facilitate opening of β-sheet A (*18*, *51*). We have previously used a fluorescent-labeled derivative of PAI-1 to demonstrate the formation of a reversible Michaelis complex between PAI-1 and the inactive S195A mutant of t-PA that cannot form covalent acyl−enzyme complexes (*44*). To test whether any overall conformational changes may be involved with the noncovalent binding of 7-ATrp PAI-1 to t-PA, emission spectra were recorded in the absence and presence of (S195A)t-PA. No significant changes in fluorescence were observed, suggesting that either formation of the Michaelis complex does not induce an overall conformational change in PAI-1 or the local environments of the 7-ATrp residues are not changed significantly (Figure 7A).

We have previously shown that the octapeptide Ac-TVASSSTA, which is composed of PAI-1 RCL residues P14−P7, competes with insertion of the RCL as strand s4A of β-sheet A and converts PAI-1 into a substrate (*52*). Reaction of 7-ATrp PAI-1 with a 100-fold excess of octapeptide results in a conversion of greater than 95% of the active 7-ATrp PAI-1 into a substrate without any generation of latent 7-ATrp PAI-1 (data not shown). Insertion of the octapeptide into β-sheet A of 7-ATrp PAI-1 results in a fluorescence quench of 23.9 ± 2.6%, in agreement with the observations of t-PA in complex with 7-ATrp PAI-1 and 7-ATrp PAI-1 cleaved by elastase (Figure 7B). Taken together with the above data for elastase cleavage, these data indicate that the observed change in fluorescence probably represents the opening of β-sheet A strands s3A and s5A to accommodate the RCL as an additional β-sheet strand.

Spontaneous Reactive Center Loop Insertion Observed by SDS-PAGE and Fluorescence. To determine whether incorporation of 7-ATrp affects the rate of spontaneous loop insertion, we evaluated the inhibitory activity over time for 7-ATrp PAI-1 and wtPAI-1 (Figures 8A,B). Reactants were incubated at 25 °C and aliquots reacted with a 2-fold molar excess of t-PA prior to SDS-PAGE analysis. Time courses

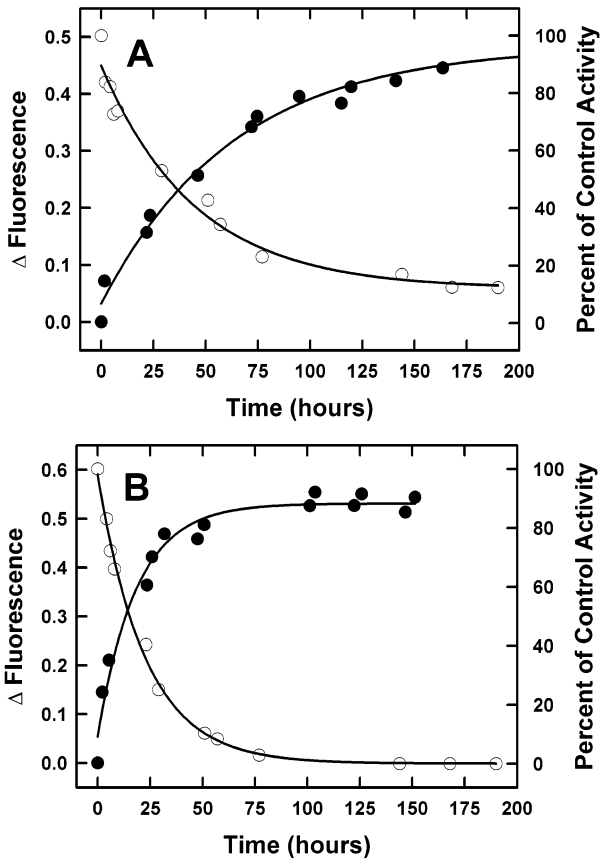

FIGURE 8: Spontaneous conversion of 7-ATrp PAI-1 and wtPAI-1 from an active to a latent conformation. Left axis (●), transition to the latent conformation was followed by fluorescence change as a function of time for 7-ATrp PAI-1 (excitation at 315 nm, panel A) and wtPAI-1 (excitation at 295 nm, panel B), as described in the Experimental Procedures. Right axis (○), transition to the latent conformation was followed by monitoring the loss of inhibitory activity against t-PA as a function of time for 7-ATrp PAI-1 (panel A) and wtPAI-1 (panel B), as described in the Experimental Procedures.

monitoring formation of the acyl−enzyme complex of 7-ATrp PAI-1 with t-PA followed a single-exponential decay with a calculated $t_{1/2}$ of 29.6 ± 1.7 h, longer than the observed $t_{1/2}$ for wtPAI-1 of 17.8 ± 2.4 h. Typically, a small fraction of 7-ATrp PAI-1 activity remained after an extended incubation at 25 °C (>300 h) that retained the ability to form SDS-stable acyl−enzyme complexes with t-PA (Figure 8A). This phenomenon was not observed with wtPAI-1 at 25 °C and may represent a small sub-population of 7-ATrp PAI-1 molecules that have an alternative folding state. Nevertheless, the majority of the 7-ATrp PAI-1 (≥90%) followed single-exponential decay kinetics indicating a single species of 7-ATrp PAI-1.

Spontaneous loop insertion was also monitored by changes in 7-ATrp and Trp fluorescence over time for 7-ATrp PAI-1 and wtPAI-1, respectively. Spontaneous transition of 7-ATrp PAI-1 to the latent species resulted in a 39.8 ± 3.0% quench of fluorescence (Figure 7A). The change in fluorescence is nearly twice that observed for cleaved loop inserted PAI-1, which has a similar crystal structure to that of the latent PAI-1 (*53*, *54*). This observation implies that the change in 7-ATrp fluorescence reflecting loop insertion also corresponds to overall conformational changes in the molecule occurring simultaneously and is sensitive to small confor-

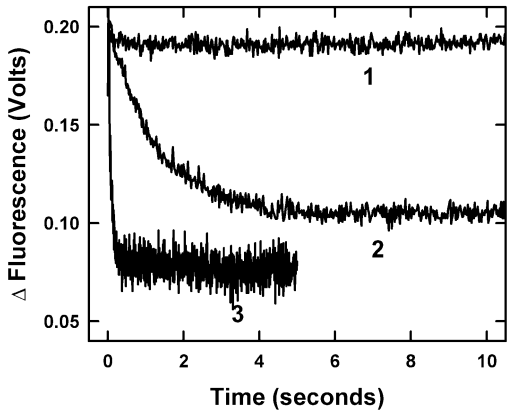

FIGURE 9: Kinetics of the serpin inhibition mechanism. 7-ATrp PAI-1 or peptide-blocked 7-ATrp PAI-1 (0.25 μM) was reacted with t-PA or u-PA (2 μM) in a stopped-flow reaction analyzer as described in Experimental Procedures with 1000 data points collected over a 5−20 s interval. Stopped-flow reaction traces have been normalized to the same initial starting fluorescence. Peptide-blocked 7-ATrp PAI-1 + u-PA, trace 1; 7-ATrp PAI-1 + t-PA, trace 2; 7-ATrp PAI-1 + u-PA, trace 3.

mational transitions that differ between latent PAI-1 and PAI-1 in complex with a proteinase. The observed change of fluorescence over time for 7-ATrp PAI-1 was in agreement with the activity measurements fitting to a $t_{1/2}$ of 36.9 ± 1.2 h (Figure 8A). Control fluorescence experiments with wtPAI-1 were monitored in parallel and are consistent with the activity measurements fitting to a $t_{1/2}$ of 13.6 ± 2.8 h (Figure 8B).

Kinetics of the Serpin−Proteinase Inhibition Reaction. The fluorescence measurements clearly indicated that conformational changes coincided with RCL insertion and that subtle changes in β-sheet A expansion can be monitored by the fluorescence emission change of 7-ATrp PAI-1. Thus, analogue incorporation provided a system for investigating overall structural transitions associated with the mechanism of RCL insertion during inhibition of a target proteinase. Reaction of 7-ATrp PAI-1 with varied concentrations of t-PA or u-PA under pseudo-first-order conditions resulted in a rapid decrease in 7-ATrp fluorescence emission that was well described by a single-exponential decay characteristic of a concerted structural transition without the formation of any discernible intermediates (Figure 9). Stopped-flow reactions of peptide-blocked 7-ATrp PAI-1, which already has an expanded β-sheet A due to peptide insertion (Figure 7B), resulted in no further fluorescence changes when reacted with u-PA (Figure 9). This is consistent with the hypothesis that the observed fluorescence change reflects conformational changes associated with expansion of β-sheet A, RCL insertion, and trapping of the proteinase in an inhibited acyl−enzyme complex.

The rates of conformational change for 7-ATrp PAI-1 reactions with u-PA were faster than reactions with equivalent concentrations of t-PA by at least 1 order of magnitude (Figure 9). We had previously observed that the limiting rate constant for the inhibition reaction of PAI-1 can be highly dependent on the specific target proteinase that is being inhibited (*7*, *14*, *44*). To address whether this observed variation was due to differences in the limiting rates of proteinase inhibition, the limiting rate (k_{lim}) for the inhibition reaction of 7-ATrp PAI-1 and different proteinases were determined (Figure 10 and Table 2). The results clearly

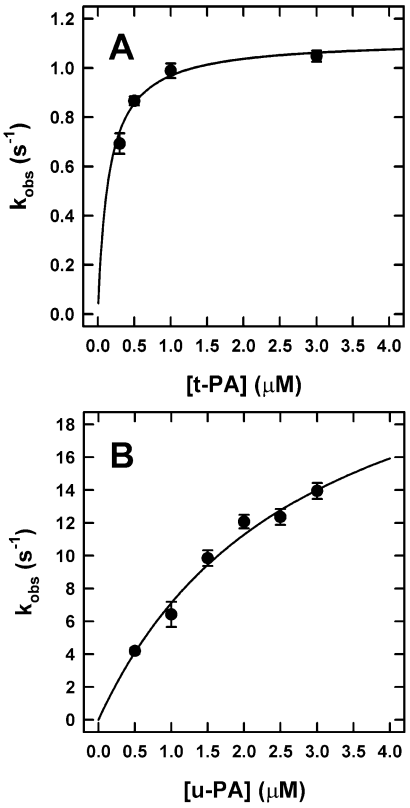

FIGURE 10: Determination of the limiting rate for proteinase inhibition. 7-ATrp PAI-1 (0.25 μM) was reacted with increasing concentrations of t-PA (A) or u-PA (B) (0.5−3.0 μM) in a stopped-flow reaction analyzer as described in Experimental Procedures. Averaged k_{obs} values from 6−10 experiments were plotted and fit to the equation of a rectangular hyperbola to obtain a k_{lim} for the reaction (Table 2). Data points are reported as an averaged value ± S.E.M.

Table 2: Rate Constants for Proteinase Inhibition by 7-ATrp PAI-1[a]

proteinase	k_{lim} (s^{-1})	K_M (μM)	k_{lim}/K_M ($M^{-1}\,s^{-1}$)
t-PA	1.1 ± 0.04	0.2 ± 0.03	5.5×10^6
u-PA	27.1 ± 3.6	2.8 ± 0.8	9.7×10^6

[a] Measured from the rapid kinetic experiments of Figure 10 in 0.03 M HEPES/0.135 M NaCl/1 mM EDTA at pH 7.4 and 25 °C. Data are reported as the best fit to the stopped-flow data ± S.E.M.

indicated a saturating dependence of the pseudo-first-order rate constants as a function of proteinase concentration with a k_{lim} of 1.1 ± 0.04 s^{-1} for t-PA and 27.1 ± 3.6 s^{-1} for u-PA. The k_{lim} value for t-PA inhibition is reduced from the limiting rate that we have previously observed for PAI-1 labeled at the P9 position with the fluorescent probe NBD (3.4 s^{-1}) (*4*).

Formation of the stable inhibited serpin−proteinase complex for the reaction of 7-ATrp PAI-1 with t-PA was directly observed using a technique independent of fluorescence. 7-ATrp PAI-1 was incubated with t-PA for various times prior to rapid acid quenching to pH 2.0, a technique which protonates His57 of the serine proteinase catalytic triad, thereby trapping the acyl−enzyme intermediate (*7*).

A time course from 0 to 10 s was sufficient to capture the complete reaction. Individual quenched reactions were analyzed by SDS-PAGE as described in the experimental procedures and plotted in Figure 11. The data fit to a limiting

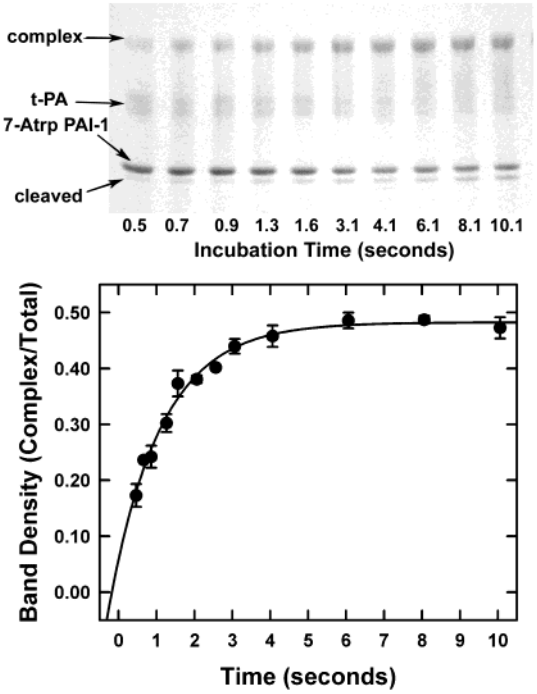

FIGURE 11: Formation of the final inhibited 7-ATrp PAI-1·t-PA complex. 7-ATrp PAI-1 (2.0 μM) was reacted with t-PA (1.0 μM) for various times from 0.5 to 10.1 s and quenched with 0.2 M HCl as described in Experimental Procedures. Data are reported as averages of at least three independent experiments ± S.E.M. and fit to the function of a first-order reaction to obtain a k_{lim} of 0.88 ± 0.09 s^{-1} for 7-ATrp PAI-1. The SDS-PAGE gel is a representative rapid acid quenching experiment. The 7-ATrp PAI-1·t-PA complex, free unreacted t-PA and 7-ATrp PAI-1, and reactive center loop cleaved 7-ATrp PAI-1 are indicated by the arrows.

rate of 0.88 ± 0.09 s^{-1}, in excellent agreement with the 1.1 s^{-1} limiting rate observed by spectroscopic techniques, demonstrating that the change in fluorescence observed in the stopped-flow experiments directly represents the trapping of the proteinase in a stable acyl−enzyme complex.

DISCUSSION

The inhibitory mechanism of serpins is characterized by an extensive conformational change following the cleavage of the scissile P1−P1′ bond and the subsequent translocation of the covalently bound proteinase from the initial position of noncovalent docking in the Michaelis complex (*12*) to the final position in an inhibited covalent serpin−proteinase complex (*9*). Our study addresses the mechanism by which serpins inhibit their target proteinases by monitoring structural transitions within the serpin by changes of the fluorescence emission of a PAI-1 mutant containing the tryptophan analogue, 7-azatryptophan. Studies that have used intrinsic tryptophan fluorescence to examine structural changes of proteins are unable to resolve transitions that occur during protein−protein interactions due to the overlapping tryptophan absorbance spectra of the interacting proteins (*22*, *55*). Biosynthetic incorporation of 7-ATrp into PAI-1 offers a distinct advantage for monitoring conformational changes by providing an intrinsic fluorescent probe that closely mimics the original amino acid without the potential problems of using tethered fluorescent molecules.

Despite their similar van der Waals radius and chemical properties, replacement of tryptophan with non-natural amino acid analogues has been shown to affect thermodynamic stability, folding, and enzymatic activity in an analogue-specific and protein-specific manner (*22*, *24*, *25*, *28*, *56*). For instance, replacement of Trp with 5-OHTrp or 5-FTrp in staphyloccal nuclease resulted in relatively insignificant changes to structure and function; yet 7-ATrp conferred a significant global destabilization in secondary structure (*25*). On the contrary, others have observed that phage lambda lysozyme was unaffected by substitution with 7-ATrp and that the incorporation of 5-FTrp into annexin V was deleterious to enzyme function (*28*, *57*). The range of variation in these observations attests to the protein-specific effects of analogue substitution but also the potential for exploiting these effects to develop a better understanding of the functional roles of tryptophan residues in a particular protein of interest. Incorporation of 7-ATrp into PAI-1 did not result in any changes to the overall secondary structure of PAI-1 (Figure 6A-B); however, we did observe a distinct proteinase specific reduction in inhibitory function and a decrease in the rate of transition to the latent conformation (Tables 1 and 2).

Kinetic Effects Due to 7-Azatryptophan Incorporation. The kinetic analyses of reactions for 7-ATrp PAI-1 inhibitions of t-PA and u-PA (Tables 1 and 2) suggested that analogue incorporation impaired inhibitory function with t-PA but not that of u-PA. This conclusion is supported by our findings that the k_{app} for inhibition of t-PA (3.3 μM^{-1} s^{-1}) is reduced 5-fold from that of the wtPAI-1 controls (15.4 μM^{-1} s^{-1}) and is primarily the result of a lower k_{lim} (1.1 s^{-1}) than that previously reported for wtPAI-1 inhibition of t-PA (3.4 s^{-1}) (*4*,*7*). Despite the effect on t-PA inhibition, we observed no effect on the inhibition of u-PA by 7-ATrp PAI-1 (Table 1). Our finding that the rate of conformational change associated with inhibition of u-PA by 7-ATrp PAI-1 (27.1 s^{-1}) greatly exceeds that for inhibition of t-PA by either 7-ATrp PAI-1 (1.1 s^{-1}) or wtPAI-1 (3.4 s^{-1}) (*4*) is evidence to support a hypothesis that the overall structural transition in the serpin inhibition mechanism is governed by a proteinase specific and rate limiting step. We attribute the large discrepancy in the overall limiting rates of reaction for t-PA and u-PA to a distinct difference in the binding interaction of the reactive center loop of PAI-1 to the active-site cleft of these proteinases. There are several possibilities that may explain this difference such as an influence on the rate of RCL cleavage, acyl−enzyme formation, or the ability of PAI-1 to efficiently separate the P′ side of the RCL from the substrate pocket after scissile bond cleavage. The latter view is in keeping with a recent report (*44*) suggesting that the rate-limiting step in the serpin inhibition mechanism could be the removal of the distal P′ side of the RCL from the substrate binding cleft of the proteinase, which, in the case of t-PA inhibition by PAI-1, requires breaking the exosite interactions between the negatively charged P4′ residue of the distal reactive center loop and the positively charged surface loop of t-PA (*58*, *59*). The corresponding surface loop on u-PA does not have the same sequence of positively charged residues (*60*), probably precluding tight exosite interactions and resulting in rapid extraction of the distal loop from the substrate binding pocket in a manner similar to our observations with inhibition of trypsin, which does not have the surface loop (*7*, *44*). Alternatively, studies have shown that the P3 and P4 residues of a substrate are the primary

determinants of t-PA and u-PA specificity and that there are significant differences between the active-site clefts of these two proteinases which affect their interactions with target substrates (*60*−*63*). Our data demonstrating that analogue substitution affected t-PA inhibition but not that of u-PA, together with the 27-fold difference in the observed limiting rates of conformational change, are consistent with our conclusion that a rate limiting step of the proteinase−inhibitor interaction is different for the two proteinases and that this step limits the overall rate of the structural transition. These results clearly contrast with those expected if analogue substitution with 7-ATrp had an effect on the intrinsic rate of loop insertion or other conformational changes associated with the kinetic trapping of a proteinase. The kinetic effects could be due to the 7-azaindole ring of the incorporated 7-ATrp which has a pK_a of about 4.5 and would contain a polar N-7 imino nitrogen at the physiological pH used for these studies (*22*). The introduction of a polar, electronegative 7-azaindole ring at the site(s) of one or more tryptophans could likely account for the observed effects on the rate limiting step and t-PA inhibition since the typical apolar environment around a tryptophan indole ring would probably not accommodate a hydrogen bond acceptor at this position (*22*, *25*). The rate-limiting step affected by analogue substitution could be reactive center loop cleavage, acylation, extraction of the P′ side from the substrate cleft, or a combination of these processes, and it warrants further investigation. While our data does not specifically identify which of these steps may be involved, we have developed a model system in which we can isolate the rate-limiting intermediate.

Serpin Inhibition as a Concerted Structural Transition. By using the spectral properties provided by 7-ATrp substitutions of the four tryptophan residues in PAI-1, we have directly observed the global changes in serpin structure that accompany proteinase trapping and shown this to be a concerted conformational transition. Analyses of the various PAI-1 crystal structures (*14*, *29*−*32*) and fluorescent spectra of active and latent PAI-1 (*37*) suggested that upon loop insertion, there are significant changes in the solvent exposure of a number of the tryptophan residues in structurally flexible regions of the serpin molecule.

Several hypotheses have been put forward regarding the mechanism and sequence of events by which full RCL insertion proceeds. It has been proposed that there is an intermediate between the Michaelis and inhibited serpin−proteinase complexes (*64*) as well as multiple conformational changes in the serpin structure identifiable prior to the point of acylation and loop cleavage, including a preinsertion of the RCL into β-sheet A from residue P15 through residue P13 upon binding of the proteinase (*18*, *51*). Other reports have argued that a translocation of the RCL occurs upon Michaelis complex formation and prior to cleavage of the RCL (*65*, *66*). These approaches relied on specific residues labeled with fluorescent probes and may have precluded a global view of the structural changes in the topology of the serpin. Our findings do not support either of the aforementioned hypotheses that suggested a stepwise mechanism of structural changes. Instead, fluorescence and stopped-flow studies identified a single concerted conformational event throughout the serpin molecule that coincides with the kinetic trapping of the proteinase in a stable acyl−enzyme complex. Our study demonstrates that insertion of the RCL octapeptide into β-sheet A, which preserves the loop in an extracted position while at the same time simulating partial loop insertion by using an exogenous peptide, produces changes of fluorescence identical to those observed for 7-ATrp PAI-1 in complex with t-PA or with the RCL cleaved by elastase. We propose that octapeptide insertion of the proximal RCL residues, at least through P7, is necessary and sufficient to expand β-sheet A and induce the molecular rearrangements in PAI-1 observed by fluorescence to accompany loop insertion. Reaction of peptide-blocked 7-ATrp PAI-1 with a proteinase did not generate any further conformational changes of the serpin (Figure 9), suggesting that the change in structure associated with proteinase trapping was complete following peptide insertion and that the minimum number of residues to promote this transition is less than P14−P7. We also observed no change in 7-ATrp PAI-1 fluorescence when in complex with a noncatalytic active-site mutant of t-PA (Figure 7A), in agreement with other observations (*44*, *67*) that there is no preinsertion of the RCL prior to cleavage by the proteinase.

Our results indicate that the change of fluorescence represents simultaneous shifts in the microenvironments of 7-ATrp residues that directly report opening of the crevice between β-strands s3A and s5A to accept the RCL as strand s4A (Figure 7A-B). The four substituted tryptophans have different positions within the PAI-1 molecule and therefore did not permit the assignment of specific structural changes. It did allow simultaneous observation of conformational transitions in multiple structurally important regions of PAI-1 and demonstrated a single concerted transition without the generation of identifiable transient intermediates. The rate constants that characterized the observed fluorescence change during reaction with t-PA (1.1 s^{-1}) agreed well with the rate of entrapment of t-PA in the acyl−enzyme complex (0.88 s^{-1}). We suggest that a single concerted structural rearrangement of the serpin topology occurs after or concomitant with the rate-limiting step of the reaction.

Fluorescence spectroscopy of the 7-ATrp PAI-1 derivative has established that the observed changes in fluorescence are due to insertion of strand 4 into β-sheet A and are similar regardless of whether they are due to inhibition of a proteinase following reactive center loop cleavage at P1−P1′, cleavage at P3−P4 by elastase, annealing with an exogenous octapeptide of RCL residues P14−P7, or spontaneous loop insertion to form a latent species. Since the binding of the octapeptide initiated an almost identical structural change in the serpin as does full loop insertion, we propose that the initial introduction of the proximal loop residues into β-sheet A are sufficient to promote the simultaneous alterations in structure that allow the reactive center loop and the tethered proteinase to be rapidly inserted into the body of the serpin. The rate constants for the 7-ATrp spectral changes induced by interaction with t-PA or u-PA were single exponentials, indicating concerted reactions with unique limiting steps. We also demonstrated that the PAI-1 inhibition mechanism was sensitive to changes in the environment of one or more tryptophan residues, since the mutation of carbon to nitrogen reduced the inhibitory efficiency of PAI-1 against t-PA 5-fold. Kinetic studies further indicated that reaction of t-PA with 7-ATrp PAI-1 resulted in an overall rate of conformational change that was

significantly slower than the limiting rate of reaction for u-PA and PAI-1. The fact that 7-ATrp substitution caused no change in the kinetic properties of u-PA inhibition is evidence to support a conclusion that a proteinase specific limiting step may retard the conformational change rates regulating reactive center loop insertion. These studies are being continued with the goal of evaluating the contribution of each tryptophan residue to the structural changes occurring during formation of a stable acyl−enzyme complex.

ACKNOWLEDGMENT

We would like to thank Dr. Arthur G. Szabo from the Department of Chemistry, Wilfrid Laurier University, Ontario, and the members of his laboratory for thoughtful discussions and their expertise with the use of tryptophan analogues. In particular, we thank Glenn Abbott for contributions to the analogue incorporation methodology, Dr. Sue Twine and Paul Malinowski for expert technical assistance and data preparation for the CD studies, and Dr. Jenny Beckingham for contributions to the preliminary fluorescence work. We also thank Ann Marie Francis-Chmura in the laboratory of J.D.S. for excellent technical support.

NOTE ADDED AFTER ASAP POSTING

This paper first appeared on the Web with an error in the equation on page E. The correct version appeared on September 17, 2002.

REFERENCES

1. Irving, J. A., Pike, R. N., Lesk, A. M., and Whisstock, J. C. (2000) *Genome Res. 10*, 1845−1864.
2. Engh, R. A., Huber, R., Bode, W., and Schulze, A. J. (1995) *Trends Biotechnol. 13*, 503−510.
3. Whisstock, J. C., Skinner, R., Carrell, R. W., and Lesk, A. M. (2000) *J. Mol. Biol. 295*, 651−665.
4. Shore, J. D., Day, D. E., Francis-Chmura, A. M., Verhamme, I., Kvassman, J., Lawrence, D. A., and Ginsburg, D. (1995) *J. Biol. Chem. 270*, 5395−5398.
5. Egelund, R., Rodenburg, K. W., Andreasen, P. A., Rasmussen, M. S., Guldberg, R. E., and Petersen, T. E. (1998) *Biochemistry 37*, 6375−6379.
6. Gils, A., and Declerck, P. J. (1998) *Thromb. Haemostasis 80*, 531−541.
7. Kvassman, J. O., Verhamme, I., and Shore, J. D. (1998) *Biochemistry 37*, 15491−15502.
8. Stratikos, E., and Gettins, P. G. (1999) *Proc. Natl. Acad. Sci. U.S.A 96*, 4808−4813.
9. Huntington, J. A., Read, R. J., and Carrell, R. W. (2000) *Nature 407*, 923−926.
10. Lawrence, D. A., Ginsburg, D., Day, D. E., Berkenpas, M. B., Verhamme, I. M., Kvassman, J. O., and Shore, J. D. (1995) *J. Biol. Chem. 270*, 25309−25312.
11. Peterson, F. C., and Gettins, P. G. (2001) *Biochemistry 40*, 6284−6292.
12. Ye, S., Cech, A. L., Belmares, R., Bergstrom, R. C., Tong, Y., Corey, D. R., Kanost, M. R., and Goldsmith, E. J. (2001) *Nat. Struct. Biol. 8*, 979−983.
13. Lawrence, D. A., Olson, S. T., Palaniappan, S., and Ginsburg, D. (1994) *J. Biol. Chem. 269*, 27657−27662.
14. Lawrence, D. A., Olson, S. T., Muhammad, S., Day, D. E., Kvassman, J. O., Ginsburg, D., and Shore, J. D. (2000) *J. Biol. Chem. 275*, 5839−5844.
15. Lee, C., Maeng, J. S., Kocher, J. P., Lee, B., and Yu, M. H. (2001) *Protein Sci. 10*, 1446−1453.
16. Stratikos, E., and Gettins, P. G. (1998) *J. Biol. Chem. 273*, 15582−15589.
17. Futamura, A., Stratikos, E., Olson, S. T., and Gettins, P. G. (1998) *Biochemistry 37*, 13110−13119.
18. Luo, Y., Zhou, Y., and Cooperman, B. S. (1999) *J. Biol. Chem. 274*, 17733−17741.
19. Olson, S. T., Swanson, R., Day, D., Verhamme, I., Kvassman, J., and Shore, J. D. (2001) *Biochemistry 40*, 11742−11756.
20. Sherman, P. M., Lawrence, D. A., Verhamme, I. M., Paielli, D., Shore, J. D., and Ginsburg, D. (1995) *J. Biol. Chem. 270*, 9301−9306.
21. Gibson, A., Baburaj, K., Day, D. E., Verhamme, I., Shore, J. D., and Peterson, C. B. (1997) *J. Biol. Chem. 272*, 5112−5121.
22. Ross, J. B., Szabo, A. G., and Hogue, C. W. (1997) *Methods Enzymol. 278*, 151−190.
23. Wong, C. Y., and Eftink, M. R. (1997) *Protein Sci. 6*, 689−697.
24. Wong, C. Y., and Eftink, M. R. (1998) *Biochemistry 37*, 8938−8946.
25. Wong, C. Y., and Eftink, M. R. (1998) *Biochemistry 37*, 8947−8953.
26. Broos, J., ter Veld, F., and Robillard, G. T. (1999) *Biochemistry 38*, 9798−9803.
27. Li, J., Szittner, R., and Meighen, E. A. (1998) *Biochemistry 37*, 16130−16138.
28. Minks, C., Huber, R., Moroder, L., and Budisa, N. (1999) *Biochemistry 38*, 10649−10659.
29. Debrock, S., and Declerck, P. J. (1998) *Thromb. Haemostasis 79*, 597−601.
30. Sharp, A. M., Stein, P. E., Pannu, N. S., Carrell, R. W., Berkenpas, M. B., Ginsburg, D., Lawrence, D. A., and Read, R. J. (1999) *Struct. Fold. Des. 7*, 111−118.
31. Nar, H., Bauer, M., Stassen, J. M., Lang, D., Gils, A., and Declerck, P. J. (2000) *J. Mol. Biol. 297*, 683−695.
32. Stout, T. J., Graham, H., Buckley, D. I., and Matthews, D. J. (2000) *Biochemistry 39*, 8460−8469.
33. Aertgeerts, K., De Bondt, H. L., De Ranter, C. J., and Declerck, P. J. (1995) *Nat. Struct. Biol. 2*, 891−897.
34. Budisa, N., Huber, R., Golbik, R., Minks, C., Weyher, E., and Moroder, L. (1998) *Eur. J. Biochem. 253*, 1−9.
35. Moran, G. R., Phillips, R. S., and Fitzpatrick, P. F. (1999) *Biochemistry 38*, 16283−16289.
36. Sambrook, J. E., Fritsch, E. F., and Maniatis, T. (1989) *Molecular Cloning: A Laboratory Manual*, Cold Spring Harbor Laboratory, Cold Spring Harbor, NY.
37. Kvassman, J.-O., and Shore, J. D. (1995) *Fibrinolysis 9*, 215−221.
38. Vaughan, D. E., Declerck, P. J., Reilly, T. M., Park, K., Collen, D., and Fasman, G. D. (1993) *Biochim. Biophys. Acta 1202*, 221−229.
39. Bradford, M. M. (1976) *Anal. Biochem. 72*, 248−254.
40. Weiss, M., Manneberg, M., Juranville, J. F., Lahm, H. W., and Fountoulakis, M. (1998) *J. Chromatogr. A 795*, 263−275.
41. Zhang, Q. S., Shen, L., Wang, E. D., and Wang, Y. L. (1999) *J. Protein Chem. 18*, 187−192.
42. Tian, W. X., and Tsou, C. L. (1982) *Biochemistry 21*, 1028−1032.
43. Hood, D. B., Huntington, J. A., and Gettins, P. G. (1994) *Biochemistry 33*, 8538−8547.
44. Olson, S. T., Swanson, R., Day, D., Verhamme, I., Kvassman, J., and Shore, J. D. (2001) *Biochemistry 40*, 11742−11756.
45. Strandberg, L., Lawrence, D. A., Johansson, L. B., and Ny, T. (1991) *J. Biol. Chem. 266*, 13852−13858.
46. Manning, M. C., and Woody, R. W. (1989) *Biochemistry 28*, 8609−8613.
47. Sherman, P. M., Lawrence, D. A., Yang, A. Y., Vandenberg, E. T., Paielli, D., Olson, S. T., Shore, J. D., and Ginsburg, D. (1992) *J. Biol. Chem. 267*, 7588−7595.
48. Gils, A., and Declerck, P. J. (1997) *J. Biol. Chem. 272*, 12662−12666.
49. Backovic, M., Stratikos, E., Lawrence, D. A., and Gettins, P. G. (2002) *Protein Sci. 11*, 1182−1191.
50. Wu, K., Urano, T., Ihara, H., Takada, Y., Fujie, M., Shikimori, M., Hashimoto, K., and Takada, A. (1995) *Blood 86*, 1056−1061.
51. Gooptu, B., Hazes, B., Chang, W. S., Dafforn, T. R., Carrell, R. W., Read, R. J., and Lomas, D. A. (2000) *Proc. Natl. Acad. Sci. U.S.A. 97*, 67−72.
52. Kvassman, J. O., Lawrence, D. A., and Shore, J. D. (1995) *J. Biol. Chem. 270*, 27942−27947.
53. Mottonen, J., Strand, A., Symersky, J., Sweet, R. M., Danley, D. E., Geoghegan, K. F., Gerard, R. D., and Goldsmith, E. J. (1992) *Nature 355*, 270−273.
54. Aertgeerts, K., De Bondt, H. L., De Ranter, C., and Declerck, P. J. (1995) *Proteins 23*, 118−121.

55. Hogue, C. W., and Szabo, A. G. (1993) *Biophys. Chem. 48*, 159−169.
56. Picking, W. D., McCann, J. A., Nutikka, A., and Lingwood, C. A. (1999) *Biochemistry 38*, 7177−7184.
57. Soumillion, P., Jespers, L., Vervoort, J., and Fastrez, J. (1995) *Protein Eng 8*, 451−456.
58. Madison, E. L., Goldsmith, E. J., Gerard, R. D., Gething, M. J., Sambrook, J. F., and Bassel-Duby, R. S. (1990) *Proc. Natl. Acad. Sci. U.S.A. 87*, 3530−3533.
59. Madison, E. L., Goldsmith, E. J., Gething, M. J., Sambrook, J. F., and Gerard, R. D. (1990) *J. Biol. Chem. 265*, 21423-21426.
60. Sperl, S., Jacob, U., Arroyo, d. P., Sturzebecher, J., Wilhelm, O. G., Bode, W., Magdolen, V., Huber, R., and Moroder, L. (2000) *Proc. Natl. Acad. Sci. U.S.A. 97*, 5113−5118.
61. Ke, S. H., Coombs, G. S., Tachias, K., Navre, M., Corey, D. R., and Madison, E. L. (1997) *J. Biol. Chem. 272*, 16603−16609.
62. Coombs, G. S., Bergstrom, R. C., Madison, E. L., and Corey, D. R. (1998) *J. Biol. Chem. 273*, 4323−4328.
63. Renatus, M., Bode, W., Huber, R., Sturzebecher, J., Prasa, D., Fischer, S., Kohnert, U., and Stubbs, M. T. (1997) *J. Biol. Chem. 272*, 21713−21719.
64. O'Malley, K. M., Nair, S. A., Rubin, H., and Cooperman, B. S. (1997) *J. Biol. Chem. 272*, 5354−5359.
65. Mellet, P., Boudier, C., Mely, Y., and Bieth, J. G. (1998) *J. Biol. Chem. 273*, 9119−9123.
66. Mellet, P., and Bieth, J. G. (2000) *J. Biol. Chem. 275*, 10788−10795.
67. Peterson, F. C., Gordon, N. C., and Gettins, P. G. (2000) *Biochemistry 39*, 11884−11892.

BI025967P